

Neuron, Volume 99

Supplemental Information

A Distance-Dependent Distribution

of Presynaptic Boutons Tunes

Frequency-Dependent Dendritic Integration

Federico W. Grillo, Guilherme Neves, Alison Walker, Gema Vizcay-Barrena, Roland A. Fleck, Tiago Branco, and Juan Burrone

Figure S1

P22

P100

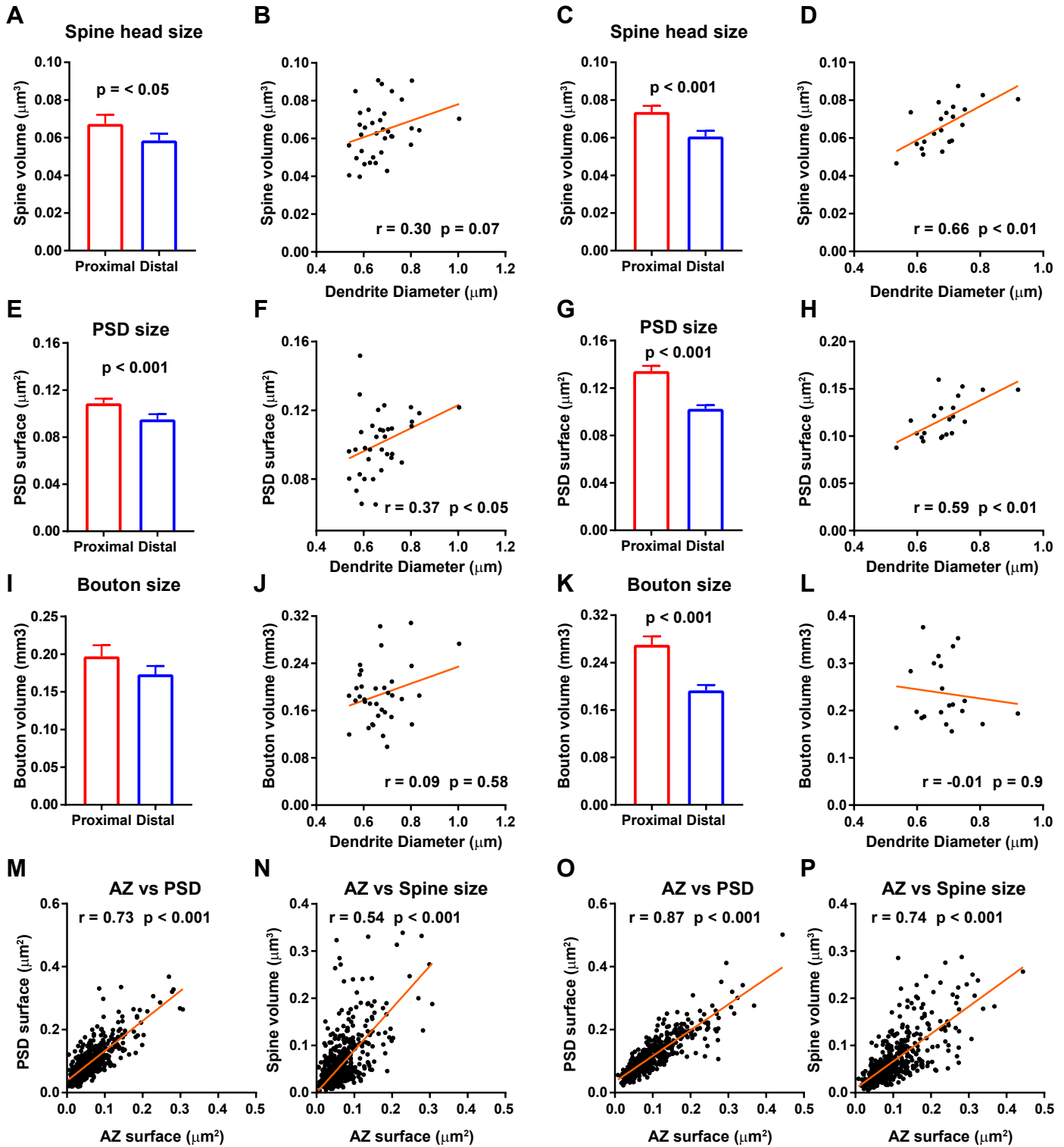
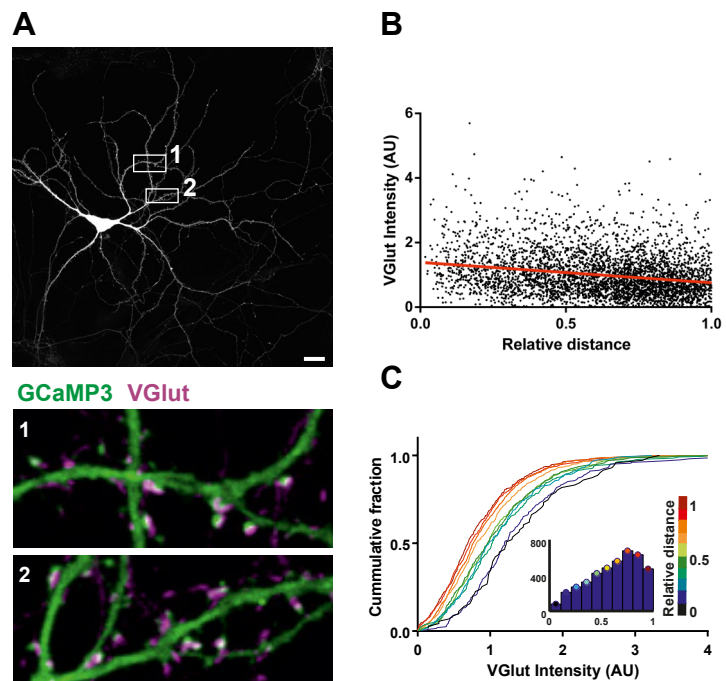


Figure S1. Synaptic properties for P22 and P100 dendrites reconstructed by SBFSEM. Related to Figure 1. For all P22 mice, N = 35 dendrites, 604 synapses. For P100 mice, N = 26 dendrites, 505 synapses. **(A-D)** Postsynaptic spine volume is smaller in distal dendrites compared to proximal dendrites in P22 and P100 mice (Wilcoxon Rank-Sum for A and C; Spearman's correlation for B and D). **(E-H)** Postsynaptic density (PSD) is smaller in distal dendrites compared to proximal dendrites in P22 and P100 mice (Wilcoxon Rank-Sum for E and G; Spearman's correlation for F and H). **(I-L)** Presynaptic bouton size (volume) in distal dendrites compared to proximal dendrites in P22 and P100 mice (Wilcoxon Rank-Sum for I and K; Spearman's correlation for J and L). **(M-P)** Correlations between PSD and AZ size (M and O, Spearman's correlation) and between spine volume and AZ size (N and P, Spearman's correlation) in P22 and P100 mice.

Figure S2

VGlut1



FM 4-64

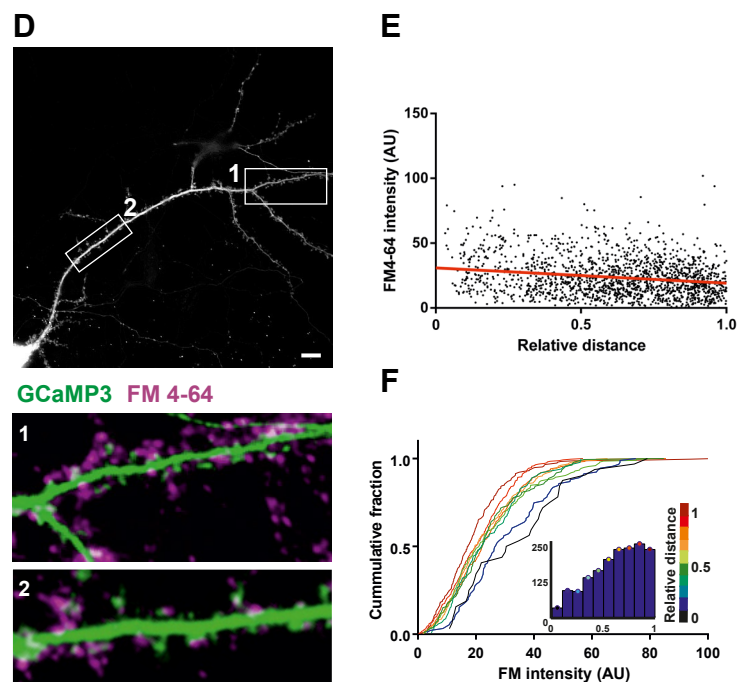


Figure S2. Preynaptic structure and function scales inversely with relative distance along a dendrite in dissociated neurons. Related to Figure 2. (A-C) Immunocytochemical labelling of vGlut1. **(A)** Example hippocampal neurons expressing GCaMP3, used here as a cytoplasmic marker. White box corresponds to the areas shown in the zoomed region below, numbered appropriately. Scale bars = 10 μm . Zoomed regions show immunostain (magenta) overlaid onto the GCaMP3 expressing cell (green). **(B)** vGlut immunostain intensity for each puncta plotted as a function of relative dendritic distance to the soma. Spearman's correlation ($P < 0.0001$, $R^2 = 0.94$, $n = 4051$ from 4 cells). **(C)** Cumulative frequency distributions for immunostain intensity for each puncta where each plot is colour-matched to a different bin for relative distance shown in the key to the right. Inset histograms show the number of spines included within each relative distance bin. **(D-F)** Labelling of vesicle recycling with FM4-64. **(D)** Example hippocampal neurons expressing GCaMP3. White box corresponds to the areas shown in the zoomed region below, numbered appropriately. Scale bars = 10 μm . Zoomed regions show FM4-64 stain (magenta) overlaid onto the GCaMP3 expressing cell (green). **(E)** FM4-64 label intensity for each puncta plotted as a function of relative dendritic distance to the soma. Spearman's correlation ($P = 0.001$, $R^2 = 0.85$, $n = 1650$ spines from 7 cells). **(F)** Cumulative frequency distributions for FM4-64 intensity for each puncta where each plot is colour-matched to a different bin for relative distance shown in the key to the right. Inset histograms show the number of spines included within each relative distance bin. Relative dendritic distance was calculated as the absolute distance (shortest path to the soma) divided by the distance from the soma to the furthest branch tip, calculated using an algorithm that searches for the longest path from each ROI to a branch tip.

Figure S3

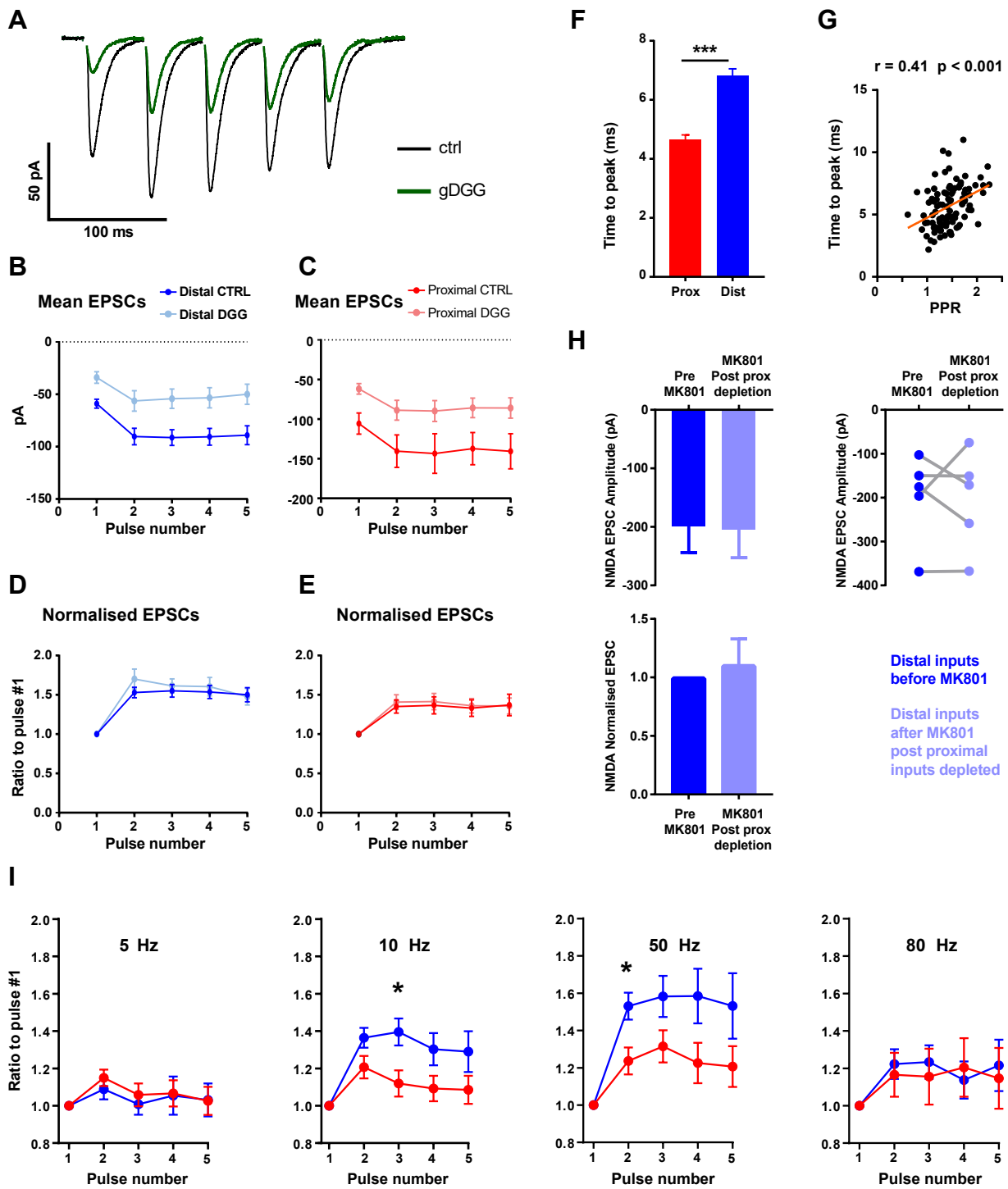


Figure S3. Physiological properties of proximal and distal synapses. Related to Figure 2. γ -D-Glutamylglycine (γ DGG) is an AMPA glutamate receptor antagonist with low affinity and fast dissociation kinetics. When present in the millimolar range it competes with released glutamate causing a reduction of AMPAR current. **(A)** EPSC amplitude is reduced, compared to control (black trace), following γ DGG application (gray trace). **(B-C)** Mean 5 pulse stimulus response amplitudes before and during 1.5 mM γ DGG bath application. **(D-E)** Normalised EPSCs for 5 pulse trains before and during 1.5 mM γ DGG bath application. Although not significant ($P = 0.15$, two-tailed paired t test) there is a small increase in PPR that is more marked in distal **(D)** compared to proximal synapses **(E)** and may reflect an increased occurrence of multi vesicular release between the first and second pulse. **(F)** The time to peak of an EPSC was significantly higher in distally triggered events (49 cells, mean = prox 6.8 ± 0.24 ms, dist 4.65 ± 0.16 ms, $p < 0.0001$ Wilcoxon sign rank test) with longer times correlating to the amount of facilitation **(G)**, Spearman's correlation. **(H)** Distal NMDAR mediated responses are not affected following blockade of proximal NMDARs with MK-801, $N=5$ cells. Top left: average amplitude of EPSCs prior to MK801 bath application (dark blue, average of 20 sweeps) and after proximal inputs have been depleted (First response to first stimulus) in MK-801 stimulation protocol (Figure 2J) (light blue); top right: changes in the amplitudes of proximal NMDAR responses for individual cells following depletion of distal NMDAR responses ($N = 5$ cells); bottom left: average NMDAR responses normalized to the response before MK-801 proximal depletion. **(I)** Facilitation over trains of 5 pulses is frequency-dependent. No statistical difference between proximal and distal responses found at 5Hz ($n = 13$ cells) and 80 Hz ($n = 9$). At 10 Hz ($n = 16$) greater distal facilitation was detected at pulse #3, $p < 0.05$; at 50 Hz ($n = 20$) greater distal facilitation was detected at pulse #2, $p < 0.05$, multiple t tests with Holm-Sidak adjusted p values.

Figure S4

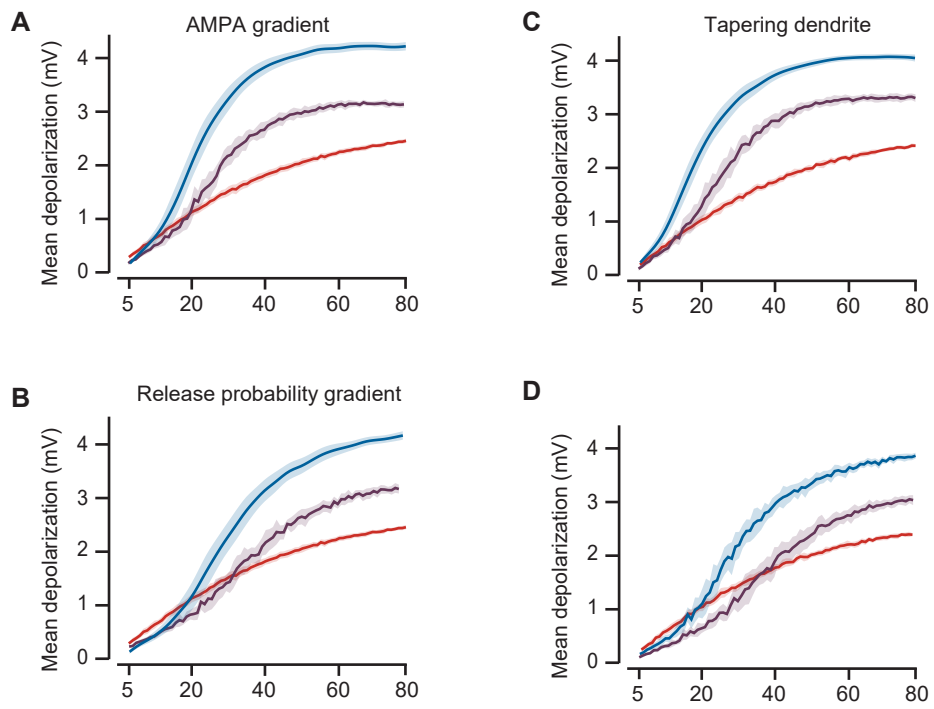


Figure S4. PPR gradient enhances distal supra-linear integration in the presence of additional gradients. Related to Figure 3. Input-output curves for models with proximo-distal gradients of **(A)** AMPA receptor conductances (distal = 81% of proximal), **(B)** release probability (distal = 70% of proximal), **(C)** dendrite diameter (distal = 85% of proximal), and **(D)** all three gradients together. For all plots red curves show proximal synapses, blue show distal synapses and purple show distal synapses with proximal PPR. Shaded area is SEM. All values for the gradients used in the model were obtained from measurements taken from Figures 1 and 2.

Supplementary text. Code for the compartmental model used in Figure 3 and S4. Compartmental model of dendritic integration that implements synaptic short-term facilitation and depression as described previously (Varela et al., 1997). Simulations were performed with the NEURON simulation environment (Hines and Carnevale, 1997).